

We are IntechOpen, the world's leading publisher of Open Access books Built by scientists, for scientists

6,900

Open access books available

186,000

International authors and editors

200M

Downloads

Our authors are among the

154

Countries delivered to

TOP 1%

most cited scientists

12.2%

Contributors from top 500 universities



WEB OF SCIENCE™

Selection of our books indexed in the Book Citation Index
in Web of Science™ Core Collection (BKCI)

Interested in publishing with us?
Contact book.department@intechopen.com

Numbers displayed above are based on latest data collected.
For more information visit www.intechopen.com



Double Perovskite $\text{Sr}_2\text{FeMoO}_6$: A Potential Candidate for Room Temperature Magnetoresistance Device Applications

Nitu Kumar, Geetika Khurana, Ram S. Katiyar,
Anurag Gaur and R. K. Kotnala

Additional information is available at the end of the chapter

<http://dx.doi.org/10.5772/intechopen.70193>

Abstract

The family of double perovskites first received attention in the 1960s, but the discovery of low field magnetoresistance (LFMR) and half metallicity of the $\text{Sr}_2\text{FeMoO}_6$ (SFMO) compound was made by Kobayashi et al. in 1998. A fully spin polarized half-metal SFMO ($T_c > 400$) with excellent magnetoresistance response relatively at small applied fields and high temperatures makes SFMO an ideal candidate for room temperature spintronics applications. Primarily, most of the research work on double perovskites SFMO has been focused on bulk ceramic samples and aimed to understand their structural, magnetic, and magnetotransport properties, along with correlation among them. A material such as SFMO that exhibits a large decrease in resistivity and magnetically order well above room temperature is necessary for the advancement of spintronic devices. If the bulk properties observed could be reproduced in thin films, industrially produced SFMO-based spintronic devices could become a reality. Therefore, the purpose of this chapter is to present the detailed background and descriptions of the double perovskite $\text{Sr}_2\text{FeMoO}_6$ (SFMO) thin films and heterostructures with main emphasis to improve or achieve room temperature magnetoresistance properties especially for room temperature magnetoresistive device applications.

Keywords: double perovskite $\text{Sr}_2\text{FeMoO}_6$, thin films, magnetic tunnel junctions, tunneling magnetoresistance

1. Introduction

Spintronics is a field of research exploiting the influence of electron spin on the electrical conduction. Spintronics materials have the unique possibilities for use in new functional

microelectronic devices and adequate potential to become the ideal memory media for computing and it is a step in the direction of quantum computing due to its advancement in nonvolatility and magnetic random access memory (MRAM). This technology could also be used to create electronic devices, which are smaller, faster and consume less power. Spintronics is one of the emerging technology, which has extended the Moore's law and industry is trying to put more than Moore. Any technology can replace the current world of electronics if it reduces any one of the very large scale integration (VLSI) cost functions like area, power consumption, speed, etc. Fortunately, spintronics can reduce heat dissipation significantly. In charge-based device to switch from logic "0" to logic "1," the magnitude of the charge must be changed in the active region of the device due to which current flows from source to drain. It is not possible with charge-based electronics to reduce the power (or heat) dissipation, since charge is a scalar quantity and the presence or absence of charge gives logic "1" or logic "0." Therefore, to meet the objective scientific community is developing the novel kind of materials that relies on magnetism instead of the flow of current through electron. The first widely acknowledged breakthrough in spintronics was the exploitation of giant magnetoresistance (GMR), a technology, which is now employed in the read heads of most hard drives. The discovery of giant magnetoresistance (GMR) has been cited as the first demonstration of a spintronics application and has been awarded the Nobel Prize in Physics in 2007 [1, 2]. GMR is a quantum mechanical effect observed in thin film heterostructures formed by alternating ferromagnetic and nonmagnetic (NM) layers. When a magnetic field (H) is applied, the thickness of NM layer is chosen such that there is a change in the direction of magnetization in another layer, which reflects a huge change in resistance. That is why the effect is called GMR, a large change in electrical resistance in presence of a magnetic field [2–4]. Baibich et al. represented the GMR of Fe/Cr magnetic superlattices by varying the magnetic field, thickness of NM (Cr) layer and by varying the number of superlattice structure [2]. They reported a large change in resistance or resistivity by applying the small magnetic field, which has a wide application in designing MRAM memories, magnetic read heads, MEMS device, etc. After that, a lot of experiments have been carried out using polarized neutron reflectometry (PNR) tool which clearly illustrates Fe/Cr superlattices that led to GMR effect [5] but PNR has some limitations also [6]. First magnetic sensor using GMR was released in 1994 [7], later, IBM produced the first GMR-read heads for reading data stored in magnetic hard disks [8, 9]. The first GMR-based RAM chips were produced by Honeywell in 1997. Today, GMR-based read heads are frequently used in laptops/computers, iPods, CD/DVD player, and other portable devices. In the twenty-first century, tunneling magnetoresistance (TMR)-based read heads began to displace GMR-based read heads. MRAM chips based on TMR devices are now marketed by several companies, such as Freescale, SanDisk, etc. Current efforts in designing and manufacturing spintronics devices is to optimize the existing GMR-based technology by either developing new materials with larger spin polarization of electrons or making improvements or variations in the existing devices that allow for better spin filtering and try to find new ways to generate and utilize the spin-polarized currents. Till date, magnetic multilayers using giant magnetoresistance (GMR) and tunneling magnetoresistance (TMR) have dominated the data storage industry

for many years using simple ferromagnetic metals such as iron and chromium. The investigation of manganite-based magnetic tunnel junctions (MTJs) has deepened our understanding of spin-polarized tunneling and the interface properties of these complex oxides. However, the initial hopes of using them for room-temperature spintronics applications have not been satisfied. Several attempts to replace current microelectronic devices with nanoscale devices have led to a search for new materials with multifunctional properties (multitasking materials that can be manipulated by independent sources). Therefore, many potential half-metallic materials have been predicted and investigated [10–19], although to date roadblocks have occurred in each case. Half-metallic materials are of great interest due to their wide variety of physical properties, including ferromagnetism, ferroelectricity, superconductivity, and many more. In the last few decades, there has been a spectacular enhancement in research activities related to doped manganites, sparked by the discovery of colossal magnetoresistance (CMR) in lanthanum-doped manganites such as $\text{La}_{1-x}\text{Ca}_x\text{MnO}_3$ [20]. The large CMR effect of the order of 10^3 percent is observed at large magnetic fields of several Tesla at low temperature. One of the first working devices using CMR materials was constructed by Sun et al. in 1996 [21]. That consists of two layers of ferromagnetic $\text{La}_{0.67}\text{Ca}_{0.33}\text{MnO}_3$ compound, separated by a thin SrTiO_3 spacer layer, which showed a resistance decreased by a factor of 2 in a field of less than 20 mT. However, the main disadvantage of this device was the grain-boundary assisted magnetoresistance properties or in ferromagnetic tunneling junctions is that the large magnetic field sensitivities are only achieved at low temperatures. Furthermore, the CMR effect vanishes far below room temperature due to their low Curie temperatures [21, 22], which make their integration to be difficult for room temperature spintronics applications. The CMR devices exploiting some of the transport properties of manganites close to room temperature have however been proposed, such as contactless potentiometers [23] or bolometers [24, 25], but none of these are strictly speaking spintronics devices. The remarkable magnetoresistive (MR) properties at low-temperature in half-metallic manganites soon motivated the search for new half-metals with higher Curie temperatures [26, 27]. Several high Curie temperature compounds have been predicted to be half-metallic in the 1980s, like semi-Heusler alloys (NiMnSb) [10, 28–31], full-Heusler alloys [32, 33], zinc-blende structure materials [34–36], magnetic oxides (e.g., rutile CrO_2 [13, 37–40] and spinel Fe_3O_4 [41, 42]). However, the first spin-polarization measurements of the Fe_3O_4 and Heusler alloys complex structures were disappointing [43]. CrO_2 has both good conductivity and high T_c , but is an unstable metastable phase that makes incorporation into devices very difficult [12]. Therefore, the half-metallic compounds with high spin polarization can dramatically enhance device performance and are required for a new generation of spintronic devices.

Much effort for the discovery of new high- T_c half-metals focused on perovskites, for which a great experience had been accumulated through the study of manganite films and heterostructures. The family of double perovskites first received attention in the 1960s [44–47], but the discovery of low-field magnetoresistance (LFMR) and half-metallicity of the $\text{Sr}_2\text{FeMoO}_6$ (SFMO) compound were investigated by Kobayashi et al. [48]. A fully spin polarized half-metal, SFMO exhibits a high Curie temperature (>400 K) and excellent magnetoresistance

response at relatively small applied fields and at high temperatures compared to manganites, making it an ideal candidate for room temperature spintronics applications.

2. Study of double perovskite $\text{Sr}_2\text{FeMoO}_6$

Primarily, most of the research works on double perovskites $\text{Sr}_2\text{FeMoO}_6$ (SFMO) has been focused on bulk ceramic samples and aimed to understand their structural, magnetic, and magnetotransport properties, along with correlation among them. The magnetoresistive (MR) properties in double perovskite SFMO generally arises from spin-dependent scattering at the grain boundaries. The underlying conduction mechanism is electron tunneling across insulating grain boundaries. Such magnetoresistance is reported to exist in polycrystalline samples in a magnetic field (~ 0.1 T), which are considerably lower fields than those utilized for manganite-based devices. The large MR, relatively at smaller external magnetic fields and at room temperature, is required in double perovskites compounds from the applications point of view. A material such as SFMO that exhibits a large decrease in resistivity and magnetically order well above room temperature is necessary for the advancement of spintronic devices.

In our studies, we had synthesized the polycrystalline $\text{Sr}_2\text{FeMoO}_6$ sample by conventional solid-state reaction method (shown in **Table 1**). In brief, the stoichiometric amounts of high purity oxides and carbonates, such as SrCO_3 , Fe_2O_3 , and MoO_3 , were mixed thoroughly as per above-mentioned formula and calcined at 900°C in Argon (Ar) for 10 h. The calcined powder were reground and pressed into thin pellets of uniform size and sintered at 1200°C for 10 h in a gas flow of 5% H_2 and 95% Ar. The details of the have been provided in our earlier reports [49–52].

Figure 1 shows the rietveld fitted X-ray diffraction patterns of the polycrystalline $\text{Sr}_2\text{FeMoO}_6$ sample, which confirm the phase purity of the samples without any observable impurity phases. All the observed peaks of double perovskite phase are clearly visible with significant presence of ordering (103, 211) peaks.

Figure 2 shows the scanning electron micrographs with elemental analysis done at two regions: one at the grain and another at the grain boundary, represented by A and B. The Fe/Mo content ratio calculated through EDS results are 94% at the grain and 93% at grain boundary for SFMO sample, which show the good correlation.

Magnetoresistance versus applied magnetic field plots for $\text{Sr}_2\text{FeMoO}_6$ samples are shown in **Figure 3** at 300 and 77 K, respectively. The MR values were calculated by using formula, $\text{MR} = 100 \times [\rho(\text{H}) - \rho(0)]/\rho(0)$, where $\rho(0)$ and $\rho(\text{H})$ are the resistivity of sample without and with magnetic field, respectively. The pristine $\text{Sr}_2\text{FeMoO}_6$ sample shows nearly 11 and 22% magnetoresistance values at 300 and 80 K, respectively, at an applied field 0.72 T. The observed 11% magnetoresistance value at room temperature at 0.72 T magnetic fields confirms the good quality of samples. High LFMR values observed in the pristine SFMO sample may be due to the optimization of intergranular (grain boundaries) and intragranular (domain walls and antisite ordering defects) barrier conditions. However, the role of intergranular barriers has the main contribution in magnetoresistance properties for double perovskite $\text{Sr}_2\text{FeMoO}_6$ compound [52–54].

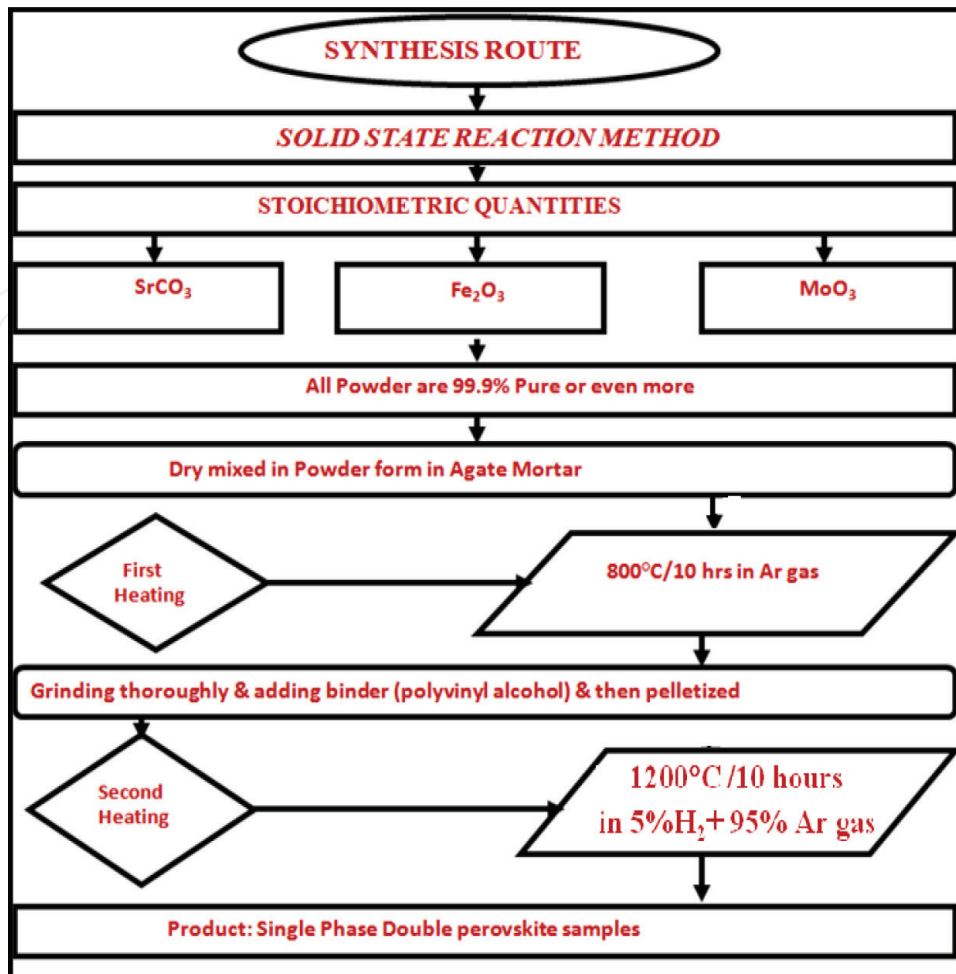


Table 1. Flow chart for the synthesis of $\text{Sr}_2\text{FeMoO}_6$ compound.

The observation of high LFMR in such double perovskite system is due to the optimization of the high spin polarization of the carriers and grain boundary adjustment. Recent studies propose a new type of MR, where the spin polarization of grain boundaries is more crucial than the

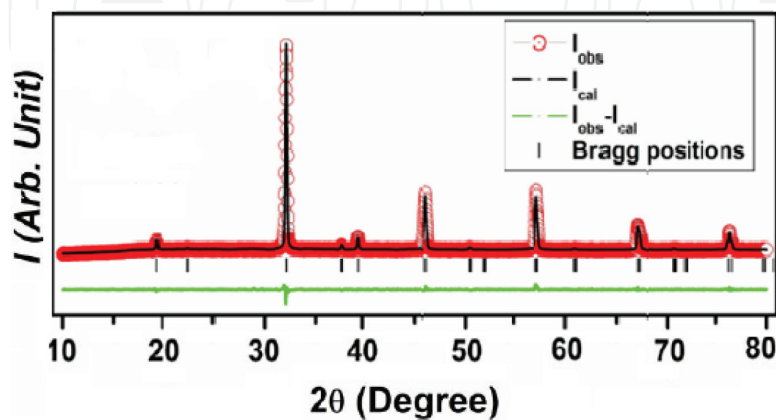


Figure 1. Rietveld fitted X-ray diffraction pattern of the samples $\text{Sr}_2\text{FeMoO}_6$.

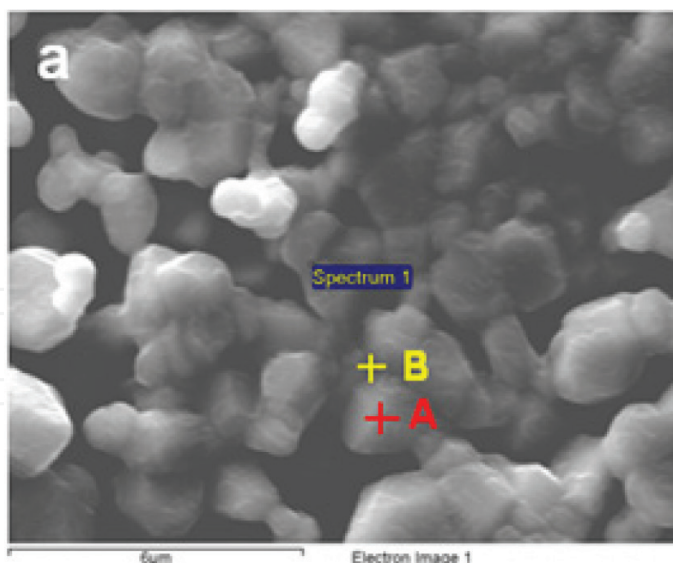


Figure 2. Scanning electron micrographs of $\text{Sr}_2\text{FeMoO}_6$ sample. A and B represents the regions where EDS pattern has been recorded at the grain and grain boundaries.

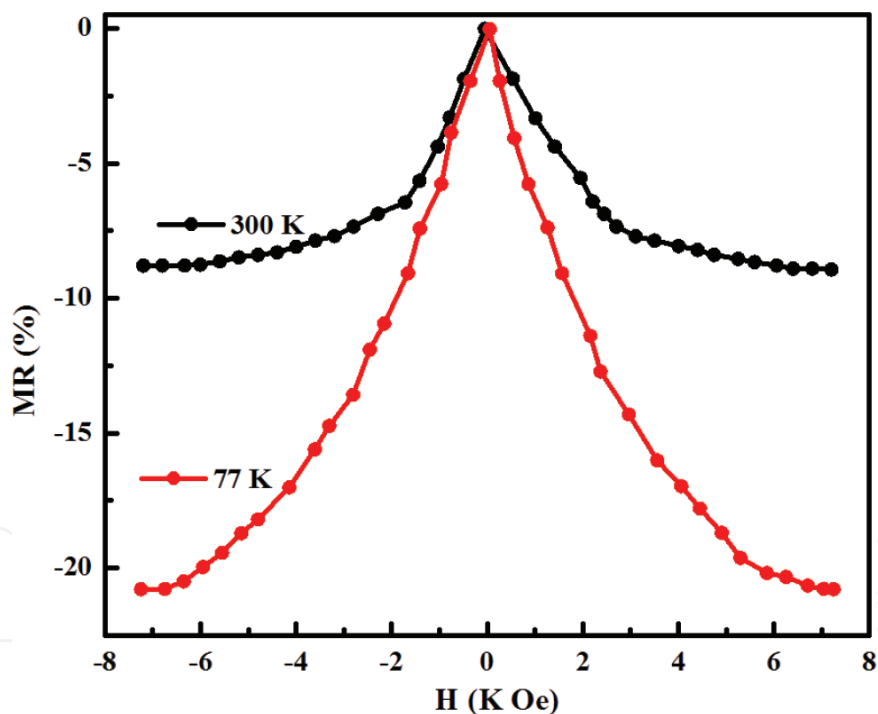


Figure 3. MR plots for the $\text{Sr}_2\text{FeMoO}_6$ at 300 and 77 K.

bulk polarization of samples [53, 55, 56]. Furthermore, the grain boundaries are magnetically hard compared to bulk in such double perovskite, which provides a different magnetic switching field for magnetoresistance and magnetization. The different behavior of the curves for normalized $(M/M_s)^2$ versus magnetic field (H) and normalized MR versus H can be observed as one of the indication of such magnetically hard nature of grain boundaries. In our pristine

sample such MR does not follow $(M/M_s)^2$, rather $(M/M_s)^2$ versus H curve saturate sharply compared to MR versus H curve, which suggest a MR mechanism similar to as reported by Sarma et al. [53]. Moreover, we estimated the low field behavior of MR and coercive field from magnetization M (μ_B /f.u.) plot and found that the peak in MR is invariably several times larger than the value of coercive field (H_c) for pristine Sr₂FeMoO₆ samples as described by Sarma et al. [53, 56]. This suggests that intragrain properties are not the key determinants for this MR. A remarkable 11% magnetoresistance was observed at room temperature under the presence of low magnetic field (0.72 T). The achieved low-field magnetoresistance value in the sample may be due to the optimized synthesis conditions to get better intergranular tunneling through grain boundaries.

3. SFMO thin films and magnetic tunnel junctions for room temperature magnetoresistive devices

Ultimately, if the bulk properties observed could be reproduced in thin films; industrially produced SFMO-based spintronic devices could become a reality. The most used and optimized method for the growth of SFMO thin film is pulsed laser deposition (PLD) [57–71], however due to inherent complexity of SFMO, its growth as a thin film, has proven to be an arduous task. A brief look through the vast array of SFMO thin film literature reveals that the growth conditions are still in need of perfection [72–83]. The substrate temperature, vacuum, oxygen partial pressure, and gas atmosphere vary from one reference to the next, making it difficult to ascertain the optimal set of growth conditions for SFMO thin films. In the very first study, Manako et al. [71] presented the effect of oxygen pressure and substrate temperature in order to get epitaxial SFMO on SrTiO₃ substrates. The phase diagram reported by them demonstrated only a narrow range of oxygen pressures (10^{-5} to 10^{-6} Torr) and temperature higher than 900°C (which is not easy to access by PLD) lead to single-phase, good quality thin films. In contrast, Santiso et al. [72] also grown the SFMO thin films and studied the effect of growth conditions, but found the formation of secondary impurity phases at high growth temperatures. Their results showed that the growth of SFMO thin films at 950°C in ultra-high vacuum (pressure less than 10^{-8} mbar), metallic iron precipitates can form, whereas in a flow of oxygen (pressure of 10^{-6} mbar), iron oxides can be formed. *In situ* X-ray photoelectron spectroscopy (XPS) analysis confirms the presence of secondary phases including SrMoO₄ and SrFeO₃ on the samples grown at lower pressures (above 10^{-4} mbar). Borges et al. [75] have also grown the SFMO thin films on SrTiO₃ substrate at different temperatures and reported significant increment in saturation magnetization (M_s) (1.4–3.5 μ_B /f.u.) by increasing the growth temperature from 770 to 950°C. Similar growth conditions were also used for films grown on slightly larger lattice mismatched MgO substrates. The saturation magnetizations for films were significantly lower than those grown on SrTiO₃. These results indicate a direct correlation between substrate temperature and degree of lattice mismatch. In comparison, Song et al. [83] determined that antisite ordering and saturation magnetization were maximized for films grown at 850°C ($M_s = 3 \mu_B$ /f.u.). However, substrate temperatures below 850°C and exceeding 900°C resulted in films with a considerable amount of antisite disorder

defects. The influence of substrate temperature upon the degree of ordering has also been demonstrated in several studies. While, Westerburg et al. [70] have been able to achieve the highest saturation magnetization (M_s) close to the ideal theoretical value of $M_s = 4 \mu_B/\text{f.u.}$ for SFMO thin film using combination of high and low growth temperature in PLD. Recently, Venimadhav et al. [73, 74] also obtained ideal value of saturation magnetization $M_s = 4 \mu_B/\text{f.u.}$ at high growth temperature of 960°C by using the mixture of reducing and oxidizing (O_2 and Ar) atmospheres. It is apparent that the substrate temperature and atmosphere conditions have a large impact on the ordering of SFMO films and should be coupled together to achieve high-quality SFMO thin films.

Another important factor that can affect crystalline quality of the SFMO films is the choice of substrate. The most admired and used substrate for growing SFMO films is SrTiO_3 (100) due to the close lattice matching [71, 77, 81, 82]. However, possible presence of oxygen vacancies [74] and low-level magnetic impurities in the SrTiO_3 substrate could lead to unusual electrical behavior, potentially causing difficulties in interpreting the data. Other substrates including MgO , LaAlO_3 [74, 80, 82, 84], and NdGaO_3 [85] have also been used to obtain epitaxial films of SFMO. There have been several studies probing the effects of lattice mismatch on the ordering and magnetization [78, 86]. Asano et al. [86] reported one of the highest magnetizations attained by depositing SFMO (via sputtering deposition) on a lattice matched buffer layer, $\text{Ba}_{0.4}\text{Sr}_{0.6}\text{TiO}_3$, then on SrTiO_3 to minimize the effect of 1% lattice mismatch between SrTiO_3 and SFMO. A considerable increase in magnetization of 2.3–3.8 $\mu_B/\text{f.u.}$ and the reduction of the expanded SFMO out-of-plane lattice parameter were observed with the use of the buffer layer. When experiments with the same buffer layer were performed by Sanchez et al. using PLD, slightly lower saturation magnetization value $\sim 3.2 \mu_B/\text{f.u.}$ was obtained [78]. In contrast, Yin et al. [80] found their magnetic and transport properties to be independent of the substrates.

The most important and challenging task is to attain good value of MR in SFMO thin films along with the structural and magnetic properties, which will make it ideal for spintronics and magnetoresistive sensors applications. However, epitaxial thin films of SFMO do not show a large MR effect due to lack of grain boundaries. As a means to obtain large MR effects, there have been attempts by varying the deposition conditions and/or the surface of substrates [63, 64, 66]. Therefore, securing a reliable means to fabricate high-quality SFMO thin films and possessing a large MR would be immensely helpful for practical device applications. Manako et al. [71] have reviewed the growth conditions of SFMO thin films, which could only be obtained in a narrow range of deposition temperature and oxygen partial pressure. They studied the magnetoresistance behavior (~ 5 and $\sim 20\%$ at 300 and 5 K, respectively) of SFMO thin films grown on SrTiO_3 (111) and (001) substrates. Their observation showed the large MR effect in (111) oriented films as compared to (001). This might suggest less scattering of carriers at grain boundaries for the (001) oriented film than for polycrystalline samples, since a perfect crystal is expected to show no MR at the temperatures far below T_c . In addition, larger MR of (111) oriented films than that of (100) oriented films may be due to the presence of antiphase domain boundaries in such a way that the superstructure direction is aligned to the growth direction. At the same time, Asano et al. [76] also deposited the $\text{Sr}_2\text{FeMoO}_{6-y}$ thin films on STO (001) substrate using two-step growth processes. The growth conditions were found to lead either highly conductive metallic thin films or semiconducting films. The metallic films show a

positive magnetoresistance (MR) as high as 35%, while the semiconducting films show a small negative MR of -3% at a temperature of 5 K and a field of 8 T. Yin et al. [80] deposited the SFMO epitaxial thin films on LaAlO_3 and SrTiO_3 (001) substrates. They defined the Wheatstone bridge arrangement straddling a bicrystal boundary to verify that the spin-dependent electron transfer is through a grain boundary or not and found that an intergranular effect is responsible for the LFMR in polycrystalline thin film samples like in the case of bulk polycrystalline samples. Song et al. [63] have also grown the SFMO thin films on SrTiO_3 substrates at optimized conditions. They found that the dominant MR mechanism operating in the SFMO films indeed spin-polarized tunneling between the magnetic grains with different orientations across the grain boundaries and concluded that it was possible to achieve a low-field MR value in the film grown at high temperature (935°C), comparable to that of a bulk sample. Shinde et al. [67] have also reported the best quality SFMO films on single-crystalline and polycrystalline SrTiO_3 substrates and found that the best quality films could only be grown at particular substrate temperature and oxygen partial pressure. According to their observation, the epitaxial film showed a very small negative MR (1.5% at magnetic field of 8 T), which is almost linear. However, the polycrystalline SFMO film also showed linear type MR behavior with magnitude around (4% at magnetic field of 8 T), which is larger than that of the epitaxial film. Some other efforts have been made to deposit the SFMO thin films in different gas environments and also postannealing treatment to achieve the LFMR by modifying the grain boundary nature [73, 78, 87]. More recently, Saloaro et al. [85] have grown the SFMO thin films on different substrates and observed the absence of traditional magnetoresistance.

Despite the large amount of research reports available for the advancement of magnetoresistance in SFMO thin films, the growth conditions vary from one reference to the next and the results are still controversial. The growth parameters including various substrates and growth temperature can directly affect the surface quality and properties. Furthermore, the fabrication of SFMO-based MTJs structure was rarely reported [61, 68, 88, 89]. There are few groups, including Bibes et al. [68], Asano et al. [88], and Fix et al. [61, 89], who have fabricated the magnetic tunnel junctions and reported the tunneling magnetoresistance (TMR) at very low temperature (5 K). However, it was noticed that the above studies mentioned the growth of MTJ on single crystalline SrTiO_3 substrates. In particular, as it was observed that one of the most important considerations for fabrication of the multilayered structure for spintronic device applications is surface/interface quality of the films. High vacuum conditions and *in situ* fabrication of multilayers is generally preferred in order to minimize the amount of secondary phase on the surface of the films. Another obstacle that can slow down the process of using these materials as a source of spin injector is the high growth temperature and complicated growth process. Furthermore, low deposition temperature and silicon substrate is required for their applications in microelectronics industry. Therefore, by considering all above aspects, firstly, we have fabricated the SFMO thin films on Si substrate by pulsed laser deposition and explored the magnetoresistance (MR) behavior besides the structural and magnetic properties. We have optimized the growth conditions and deposited the SFMO thin films at different temperatures ranging from $500\text{--}800^\circ\text{C}$ and observed the magnetotransport behavior of SFMO polycrystalline thin films grown on Strontium titanate (STO) buffered Si (100) substrate. After that, we had fabricated the SFMO/ SrTiO_3 /SFMO MTJ structure on SrTiO_3 buffered Si (100) substrate to obtain the room temperature magnetoresistance. We observed

the ~7% TMR in SFMO/STO/SFMO MTJ, which can be attributed to spin-dependent electron tunneling across the interfaces. The presented results will open up the future prospects of integration of such polycrystalline SFMO thin films for magnetoresistive applications.

A pulsed laser deposition technique was used to deposit the SFMO thin films on SrTiO₃ buffered Si (100) substrates. The experimental details are provided below.

1. To optimize the growth conditions of SFMO thin films, substrate temperatures were varied from 500 to 800°C under the base vacuum pressure higher than ($>5 \times 10^{-6}$ Torr).
2. Prior to the deposition of SFMO films, STO buffer layer was grown on Si substrate in the presence of high purity (99.99%) oxygen at an ambient pressure of ~50 mTorr at 500°C and subsequently annealed *in situ* at 800°C in O₂ pressure of ~500 mTorr.
3. After the deposition of STO buffer layer on Si (100) substrate, SFMO thin layers were deposited at fixed temperature under the base vacuum pressure ($\sim 5 \times 10^{-6}$ Torr) and subsequently annealed *in situ* at the same conditions for 10 min.
4. The temperature of substrate was ramped down at 10°C per minute after deposition to prevent thermal shock and cracking of the film.
5. In this study, we fixed all growth parameters and varied only substrate temperature to optimize the growth conditions.

Figure 4, shows the XRD patterns of SFMO thin films grown on STO buffered Si (100) substrate at four different elevated temperatures ranging from 500 to 800°C at a step of 100°C. The growth of SFMO thin film at low temperature ($\leq 600^\circ\text{C}$) do not produce the stoichiometric

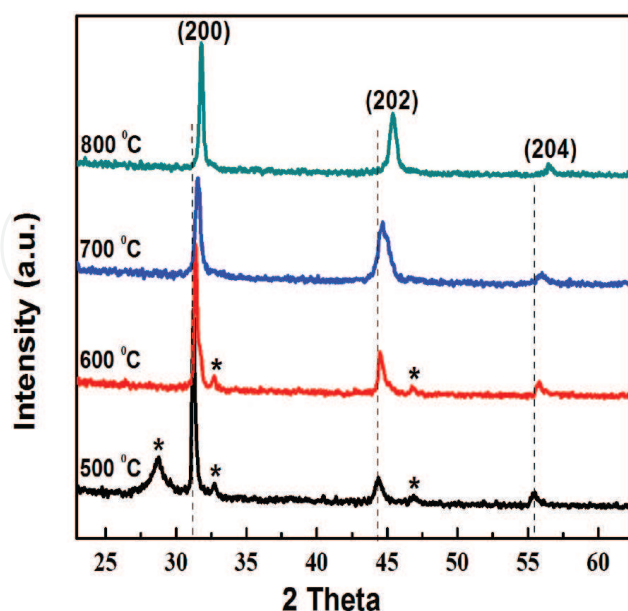


Figure 4. X-ray diffraction pattern of SFMO thin films grown on STO buffered Si (100) substrate at temperatures 500, 600, 700 and 800°C.

SFMO phase and an additional spurious peak of strontium molybdate (SrMoO_4) phase (as indicated by * in **Figure 1**) was formed. The secondary impurity phases can be commonly observed at low growth temperatures of SFMO thin films [90, 91]. These impurity phases also develop the antisite disorder in the double perovskite lattice, which further affect the magnetic and magnetotransport properties of SFMO thin films [92, 93]. However, the aforesaid impurity phases were completely disappeared, and a single phase formation of polycrystalline SFMO thin films was observed when the growth temperature was raised to 700°C and above.

The SFMO thin film grown at 800°C shows a series of peaks at $2\theta = 31.7, 45.2$ and 56.3° corresponding to the (200), (202), and (204) planes, respectively of SFMO phase, which are consistent with the results of Jalili et al. [90]. However, noticeable change in the shifting and sharpening of XRD peaks were observed with increasing growth temperature. This is apparently a consequence of the enhancement in the crystallinity of film with increasing growth temperature. A shifting of peak positions indicates that the thin films are not fully relaxed at low growth temperatures ($\leq 600^\circ\text{C}$). Therefore, we observed that the substrate temperature (T_D) plays crucial role for exact phase formation and improving the crystalline nature of SFMO films.

The magnetoresistance properties of SFMO thin films deposited at different temperatures were measured using four probe resistivity setups at magnetic field up to ± 8 T. The magnetoresistance values are 0.009, 0.017, 0.16, and 0.35% for films deposited at 500, 600, 700, and 800°C , respectively, at room temperature and magnetic field of ± 8 T as shown in **Figure 5**.

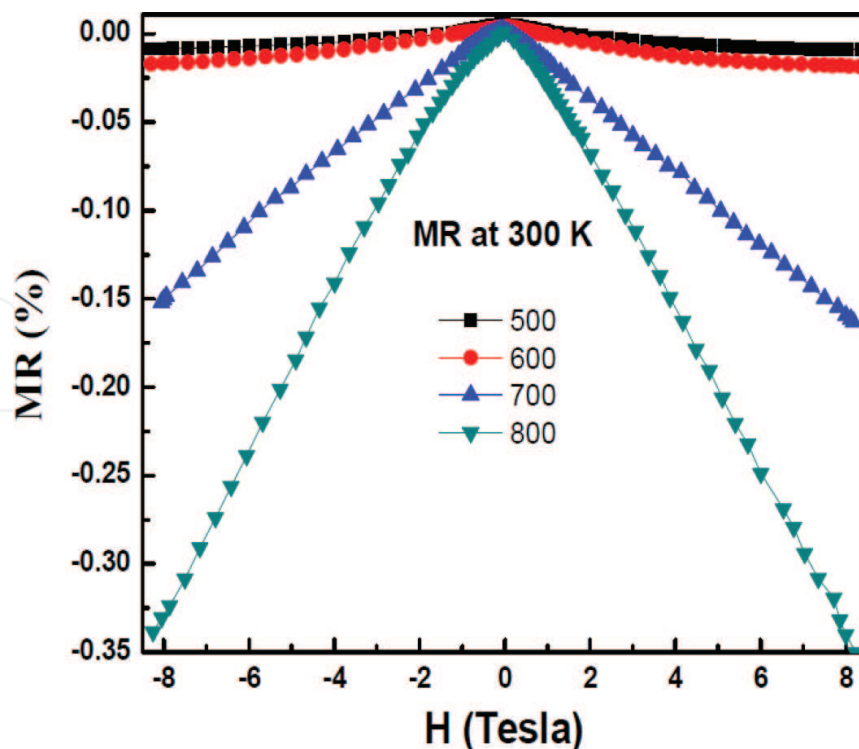


Figure 5. MR behavior of all the SFMO thin films at room temperature.

It is clearly observed that the film grown at low temperature ($\leq 600^\circ\text{C}$) exhibited the small MR effect and further it was found to be enhanced with growth temperature. This enhanced behavior of MR may be due to the improvement in the crystallinity of the intragranular nature and also by decrement in the antisite disorders effect. Improvement in structural and magnetic properties strongly supports the enhanced magnetoresistance at room temperature. The MR values are 0.35 and 12% at 300 and 5 K for polycrystalline SFMO film grown at 800°C , which shows almost linear type of behavior with magnetic field.

Pulsed laser deposition was used to fabricate SFMO/SrTiO₃/SFMO Magnetic tunnel junctions on SrTiO₃ buffered Si (100) substrate. The details of the experiments are given below.

1. In the first step, we have optimized the thickness of STO layer by controlling number of laser shots, which was estimated in separate experiments by an empirical relation of thickness and laser pulse counts.
2. The STO buffer layer was grown on Si (100) substrate in the presence of high purity (99.99%) oxygen at an ambient pressure of ~ 50 mTorr at 500°C and subsequently annealed *in situ* at 800°C in oxygen pressure of ~ 500 mTorr.
3. The STO buffer layer was characterized by X-ray diffraction technique and found to be crystalline in nature.
4. The SFMO bottom electrode has been deposited at 800°C in the base vacuum pressure higher than $\sim 5 \times 10^{-6}$ Torr and annealed *in situ* at 800°C for 10 min.
5. The crystal structure and phase purity of SFMO bottom layer was examined by X-ray diffraction and micro Raman microscopy, which shows single-phase formation of SFMO thin film without any impurity phases. The XPS analysis confirms that the Fe:Mo ratio is almost equal ($\sim 1:1.1$) over the surface of SFMO thin films.
6. Then ~ 2 nm STO barrier layer was deposited at 800°C with 5×10^{-6} Torr pressure. Again SFMO top layer was deposited at the same conditions as that of bottom SFMO electrode.
7. The shadow mask having lateral dimension $40 \mu\text{m} \times 40 \mu\text{m}$ was used during the fabrication of trilayer SFMO/STO/SFMO structure.

Figure 6(a) shows the schematic of SFMO/STO/SFMO MTJ structure as pattern on STO buffered Si (100) substrate.

The thickness of the SFMO electrodes was kept (≥ 50 nm) to insure the half-metallic nature of grown SFMO layers [64] and the thickness of STO barrier layer was kept ~ 2 nm to examine the tunneling effect. The cross-sectional high-resolution field emission scanning electron microscopy (FESEM) image of SFMO/STO/SFMO MTJ structure grown on STO buffered Si (100) substrate as shows in **Figure 6(b)**. The thickness of STO buffer layer is (~ 10 nm), which is grown on Si substrate. The presence of (~ 2 nm) STO barrier layer is clearly seen by bright horizontal contrast in the FESEM image, which is perfectly sandwiched between top and bottom SFMO electrodes.

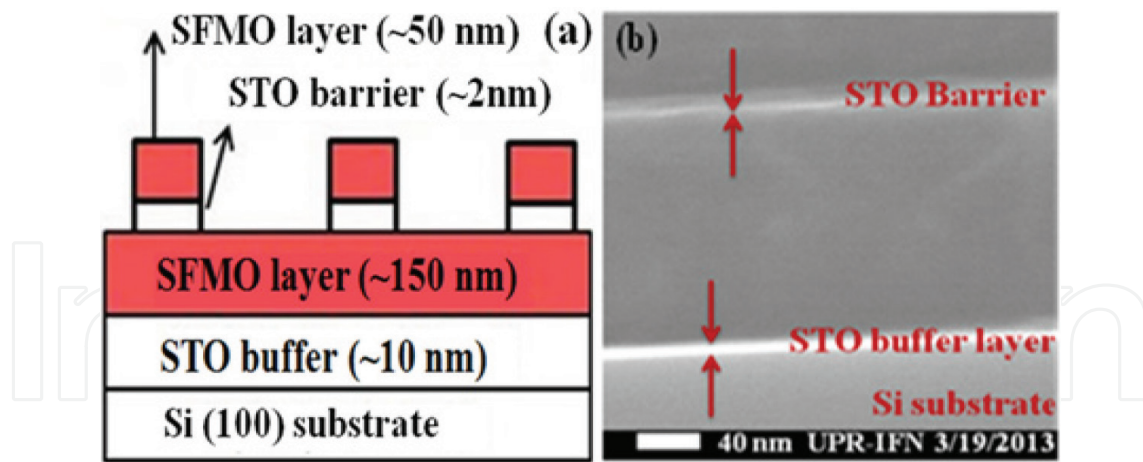


Figure 6. (a) Schematic of the typical SFMO/STO/SFMO MTJ structure. (b) Cross-sectional FESEM image of SFMO/STO/SFMO structure grown on STO buffered Si substrate at 800°C.

Figure 7(a) represents the current voltage (I-V) behavior of SFMO bottom layer and SFMO/STO/SFMO MTJ structure at room temperature. It can be seen from **Figure 7(a)** that I-V behavior of the SFMO bottom layer is almost linear while it shows nonlinear and asymmetric behavior for SFMO/STO/SFMO MTJ at room temperature. This behavior of MTJ is quite different from the SFMO electrode layer and shows the typical characteristic of tunneling assisted transport across a thin insulating barrier [68, 94]. The tunneling conductance in SFMO/STO/SFMO magnetic tunnel junction is further confirmed by fitting the conductance (dI/dV) characteristics as shown in **Figure 7(b)** using Brinkman's formula [95] intended for direct tunneling transport through a rectangular barrier. The thickness of the STO barrier layer was calculated from the fitting of the experimental data and was found to be ~1.5 nm, which is in close agreement with the estimated thickness of the STO barrier layer through FESEM image (~2 nm).

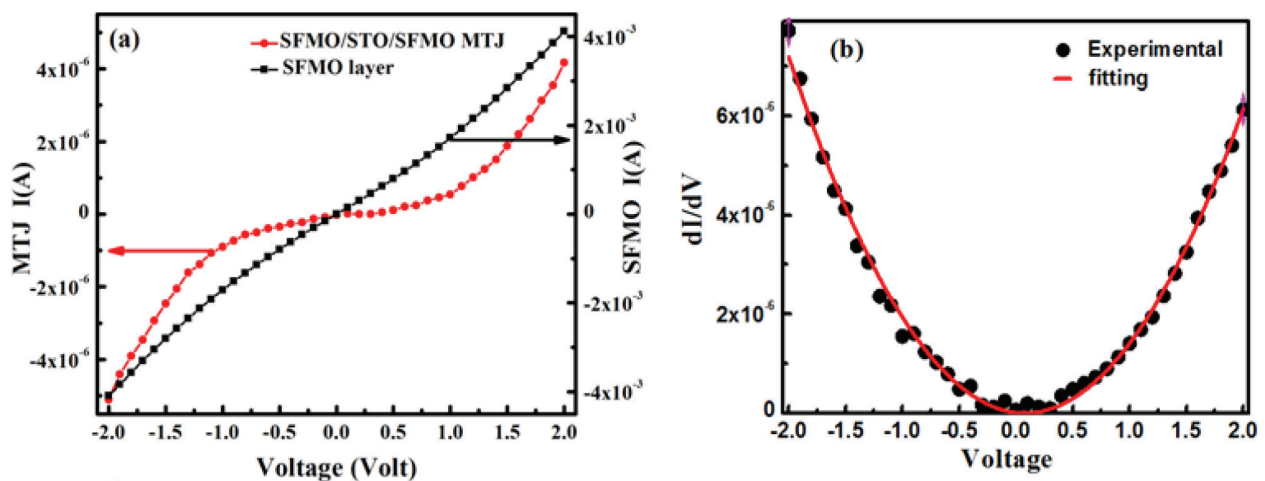


Figure 7. (a) Current-voltage characteristics of SFMO thin films and SFMO/STO/SFMO MTJ at 300 K. (b) Conductance fitting of SFMO/STO/SFMO MTJ.

Figure 8 shows the magnetic field dependence of the resistance for a SFMO/STO/SFMO MTJ with a junction area of $40 \times 40 \mu\text{m}^2$, measured at 300 K. This is defined as $(R_{\text{AP}} - R_{\text{P}})/R_{\text{P}}$, where R_{P} and R_{AP} are the resistances for parallel and antiparallel magnetic configurations of the two electrodes, respectively. When sweeping the field from negative to positive values, the resistance of the junction rises from 2.74 to 2.95 M Ω , yielding a TMR ratio of $\sim 7\%$ at 300 K.

This type of abrupt change in resistance is related to the reversal of two electrodes within the constriction as already observed in Co/I/SFMO [68] and LSMO/STO/LSMO [96] MTJ trilayer junctions fabricated using similar approach. The TMR ratio of MTJ device is related to the spin polarizations P_1 and P_2 of the two ferromagnetic electrodes as $\text{TMR} = 2P_1P_2/(1 - P_1P_2)$ using classical Julliere expression [97], where $P = P_1 = P_2$. The observed high value of spin polarization ($\sim 18\%$) at room temperature is attributed to electrons tunneling between SFMO layers through thin (~ 2 nm) insulating STO barrier. Further to confirm the TMR effect in SFMO/STO/SFMO MTJ, we have independently studied the MR behavior of SFMO film and observed a very small change in MR ($\sim 0.35\%$) at room temperature, which is quite comparable with the reported value for epitaxially grown SFMO films on STO substrate [85, 98]. Based on these results, we propose that the enhanced spin polarization and TMR in SFMO/STO/SFMO MTJ devices is due to the spin-dependant tunneling through ultra-thin insulating and atomically flat STO barrier layer sandwiched between two ferromagnetic SFMO electrodes with sharp interfaces. The sharp change in TMR at the switching field (H_s), where the magnetic moments of the SFMO electrodes realigned from parallel to antiparallel, suggests an entire flip of the magnetic domains against the applied magnetic field. However, the switching field (H_s) at 300 K is less than 30 Oe, which agrees with the coercivity (H_c) of the SFMO film. Hence, the observation of room temperature ($\sim 7\%$) TMR in SFMO/STO/SFMO MTJ can be attributed to spin dependent electron tunneling across the interfaces.

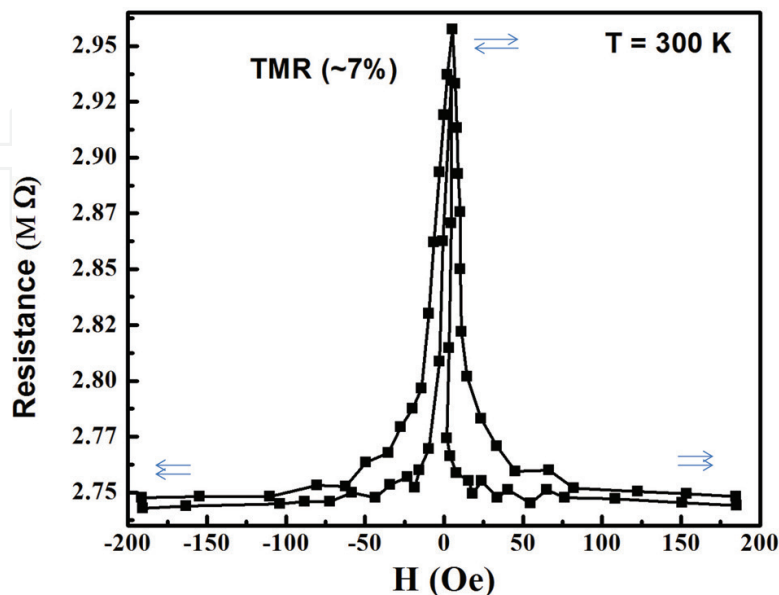


Figure 8. Magnetoresistance behavior of SFMO/STO/SFMO MTJ at 300 K.

4. Conclusions

We had synthesized and presented the double perovskite $\text{Sr}_2\text{FeMoO}_6$ bulk compound, which shows the remarkable 11% low-field magnetoresistance at room temperature at low magnetic field (0.72 T). This value is one of the high MR value at 300 K, which was only achieved due to the optimized synthesis conditions to achieve better intergranular tunneling through grain boundaries. The brief overview of the synthesis of SFMO thin films has been provided. Furthermore, low deposition temperature and silicon substrate are required for their applications in microelectronics industry; therefore, we have fabricated the SFMO thin films on Si substrate at optimized growth conditions by pulsed laser deposition. The polycrystalline $\text{Sr}_2\text{FeMoO}_6$ thin films have been grown on STO buffered Si (100) substrates. We also made an attempt to observe the room temperature magnetoresistance in $\text{Sr}_2\text{FeMoO}_6$ -based magnetic tunnel junctions (MTJ). The micrometer-sized ($\text{Sr}_2\text{FeMoO}_6/\text{SrTiO}_3/\text{Sr}_2\text{FeMoO}_6$) devices were grown by pulsed laser deposition. FESEM micrograph analysis revealed the presence of ultrathin (~2 nm) STO barrier layer. Magnetization measurements showed the good ferromagnetic loop behavior with high Curie temperature (T_c) well above 375 K. The current-voltage characteristics of the MTJ devices at room temperature exhibited nonlinear and asymmetric behavior in agreement to the predictions of tunnel conductance. The observed large tunneling magnetoresistance (TMR ~ 7%) at room temperature can be attributed to spin-dependent tunneling across a uniform ultrathin STO tunnel barrier sandwiched between two identical SFMO electrodes in MTJ devices. Finally, we showed that the polycrystalline SFMO thin films and its MTJ structures have enough potential for magnetoresistive and spintronic devices and their possible integration with existing Silicon-based microelectronic devices.

Acknowledgements

Authors acknowledge the financial support from Council of Scientific and Industrial Research Grant at National Physical Laboratory, India and DOD Grant AFOSR-FA9550-16-1-0295 at UPR, Puerto Rico.

Author details

Nitu Kumar^{1*}, Geetika Khurana¹, Ram S. Katiyar¹, Anurag Gaur² and R. K. Kotnala³

*Address all correspondence to: chauhannitu@gmail.com

1 Department of Physics, University of Puerto Rico, San Juan, Puerto Rico, USA

2 Department of Physics, National Institute of Technology, Kurukshetra, India

3 Spintronic and Magnetic Standard Group, CSIR-National Physical Laboratory, New Delhi, India

References

- [1] The Nobel Prize in Physics 2007 Albert Fert Unité Mixte de Physique CNRS/THALES, Université Paris-Sud, Orsay, France, and Peter Grünberg Forschungszentrum Jülich, Germany, "for the discovery of Giant Magnetoresistance". http://nobelprize.org/nobel_prizes/physics/laureates/2007/press.html
- [2] Baibich MN, Broto JM, Fert A, Van Dau FN, Petroff F, Eitenne P, Creuzet G, Friederich A, Chazelas J. Giant Magnetoresistance of (001)Fe/(001)Cr Magnetic Superlattices. *Physical Review Letters*. 1988;**61**:2472
- [3] Fert A. Nobel Lecture: Origin, development, and future of spintronics. *Reviews of Modern Physics*. 2008;**80**:1517
- [4] Binash G, Grünberg P, Saurenbach F, Zinn W. Enhanced magnetoresistance in layered magnetic structures with antiferromagnetic interlayer exchange. *Physical Review B*. 1989;**39**:4828
- [5] Moyerman¹ S, Eckert JC, Borchers JA, Perdue KL, Doucet M, Sparks PD, Carey MJ. Magnetic structure variations during giant magnetoresistance training in spin valves with picoscale antiferromagnetic layers. *Journal of Applied Physics*. 2006;**99**:08R505
- [6] Li M, Cui W, Yu J, Dai Z, Wang Z, Katmis F, Guo W, Moodera J. Magnetic proximity effect and interlayer exchange coupling of ferromagnetic/topological insulator/ferromagnetic trilayer. *Physical Review B*. 2015;**91**:014427
- [7] Daughton JM, Brown J, Chen E, Beech R, Pohm AV, Kude W. Magnetic field sensors using GMR multilayer. *IEEE Transactions on Magnetics*. 1994;**30**:4608
- [8] IBM Archives: IBM 350 disk storage unit. IBM. Retrieved 2011-07-20
- [9] Prinz GA. Magnetoelectronics. *Science*. 1998;**282**:1660
- [10] de Groot RA, Mueller FM, van Engen PG, Buschow KHJ. New Class of Materials: Half-Metallic Ferromagnets. *Physical Review Letters*. 1983;**50**:2024
- [11] Pickett WE, Singh DJ. Electronic structure and half-metallic transport in the La_{1-x}CaxMnO₃ system. *Physical Review B*. 1996;**53**:1146
- [12] Bibes M, Barthélémy A. Oxide spintronics. *IEEE Transactions on Electron Devices*. 2007;**54**:1003-1023
- [13] Schwarz K. CrO₂ predicted as a half-metallic ferromagnet. *Journal of Physics F: Metal Physics*. 1986;**16**:L211
- [14] Ji Y, Strijkers GJ, Yang FY, Chien CL, Byers JM, Anguelouch A, Gang Xiao and Gupta A. Determination of the Spin Polarization of Half-Metallic CrO₂ by Point Contact Andreev Reflection. *Physical Review Letters*. 2001;**86**:5585

- [15] Brabers VAM. Progress in spinel ferrite research. In: Buschow KHJ, editor. *Ferromagnetic Materials*. Vol. 8. Amsterdam: Elsevier; 1995. p. 189
- [16] Yanase A, Siratori K. Band Structure in the High Temperature Phase of Fe_3O_4 . *Journal of the Physical Society of Japan*. 1984;**53**:312
- [17] Serrate D, DeTeresa JM, Ibarra MR. Magnetoelastic coupling in $\text{Sr}_2(\text{Fe}_{1-x}\text{Cr}_x)\text{ReO}_6$ double perovskites. *Journal of Physics: Condensed Matter*. 2007;**19**:023201
- [18] Krockenberger Y, Mogare K, Reehuis M, Tovar M, Jansen M, Vaitheeswaran G, Kanchana V, Bultmark F, Delin A, Wilhelm F, Rogalev A, Winkler A, Alff L. $\text{Sr}_2\text{CrOsO}_6$: End point of a spin-polarized metal-insulator transition by 5d band filling. *Physical Review B*. 2007;**75**:020404
- [19] Miura Y, Nagao K, Shirai M. Atomic disorder effects on half-metallicity of the full-Heusler alloys $\text{Co}_2(\text{Cr}_{1-x}\text{Fe}_x)\text{Al}$: A first-principles study. *Physical Review B*. 2004;**69**:144413
- [20] Jin S, Tiefel TH, McCormack M, Fastnacht RA, Ramesh R, Chen LH. Thousandfold Change in Resistivity in Magnetoresistive La-Ca-Mn-O Films. *Science*. 1994;**264**:413
- [21] Sun JZ, Gallagher WJ, Duncombe PR, Krusin-Elbaum L, Altman RA, Gupta A, Lu Yu, Gong GQ, Xiao G. Observation of large low-field magnetoresistance in trilayer perpendicular transport devices made using doped manganate perovskites. *Applied Physics Letters*. 1996;**69**:3266
- [22] Yin HQ, Zhou JS, Goodenough JB. Near-room-temperature tunneling magnetoresistance in a trilayer $\text{La}_{0.67}\text{Sr}_{0.33}\text{MnO}_3/\text{La}_{0.85}\text{Sr}_{0.15}\text{MnO}_3/\text{La}_{0.67}\text{Sr}_{0.33}\text{MnO}_3$ device. *Applied Physics Letters*. 2000;**77**:714
- [23] Balcells LI, Cifre J, Calleja A, Fontcuberta J, Varela M, Benitez F. Room-temperature magnetoresistive sensor based on thick films manganese perovskite. *Sensors and Actuators*. 2000;**81**:64
- [24] Goyal A, Rajeswari M, Shreekala R, Lofland SE, Bhagat SM, Boettcher T, Kwon C, Ramesh R, Venkatesan T. Material characteristics of perovskite manganese oxide thin films for bolometric applications. *Applied Physics Letters*. 1997;**71**:2535
- [25] Yang CH, Koo J, Song C, Koo TY, Lee KB, Jeong YH. Resonant x-ray scattering study on multiferroic BiMnO_3 . *Physical Review B*. 2006;**73**:224112
- [26] de Teresa JM, Barthelemy A, Fert A, Contour JP, Montaigne F, Seneor P. Role of Metal-Oxide Interface in Determining the Spin Polarization of Magnetic Tunnel Junctions. *Science*. 1999;**286**:507
- [27] Pantel D, Goetze S, Hesse D, Alexe M. Reversible electrical switching of spin polarization in multiferroic tunnel junctions. *Nature Materials*. 2012;**11**:289
- [28] de Groot RA, Mueller FM, van Engen PG, Buschow KHJ. Half-metallic ferromagnets and their magneto-optical properties. *Journal of Applied Physics*. 1984;**55**:2151

- [29] Hanssen KEHM, Mijnders PE. Positron-annihilation study of the half-metallic ferromagnet NiMnSb: Theory. *Physical Review B*. 1986;**34**:5009
- [30] Galanakis I, Ostanin S, Alouani M, Dreysse H, Wills JM. Ab initio ground state and L_{2,3} x-ray magnetic circular dichroism of Mn-based Heusler alloys. *Physical Review B*. 2000;**61**:4093
- [31] Fang CM, de Wijs GA, de Groot RA. Spin-polarization in half-metals. *Journal of Applied Physics*. 2002;**91**:8340
- [32] Galanakis I. Surface Properties of the Half- and Full-Heusler Alloys. *Journal of Physics: Condensed Matter*. 2002;**14**:6329
- [33] Galanakis I, Dederichs PH, Papanikolaou N. Slater-Pauling behavior and origin of the half-metallicity of the full-Heusler alloys. *Physical Review B*. 2002;**66**:174429
- [34] Liu BG. Robust half-metallic ferromagnetism in zinc-blende CrSb. *Physical Review B*. 2003;**67**:172411
- [35] Xie WH, Xu YQ, Liu BG, Pettifor DG. Half-Metallic Ferromagnetism and Structural Stability of Zincblende Phases of the Transition-Metal Chalcogenides. *Physical Review Letters*. 2003;**91**:037204
- [36] Galanakis I. Surface half-metallicity of CrAs in the zinc-blende structure. *Physical Review B*. 2002;**66**:012406
- [37] van Lueken H, de Groot RA. Electronic structure of the chromium dioxide (001) surface. *Physical Review B*. 1995;**51**:7176
- [38] Hwang HY, Cheong SW. Enhanced Intergrain Tunneling Magnetoresistance in Half-Metallic CrO₂ Films. *Science*. 1997;**278**:1607
- [39] Korotin A, Anisimov VI, Khomskii DI, Sawatzky GA. CrO₂: A Self-Doped Double Exchange Ferromagnet. *Physical Review Letters*. 1998;**80**:4305
- [40] Tripathy D, Adeyeye AO. Electronic properties of field aligned CrO₂ powders. *Physica B*. 2005;**368**:131
- [41] de Groot RA, Buschow KH. Recent developments in half-metallic magnetism. *Journal of Magnetism and Magnetic Materials*. 1986;**54**:1377
- [42] Pénicaud M, Silberchoit B, Sommers CB, Kübler J. Calculated electronic band structure and magnetic moments of ferrites. *Journal of Magnetism and Magnetic Materials*. 1992;**103**:212
- [43] Bona GL, Meier F, Taborelli M, Bucher E, Schmidt PH. Spin polarized photoemission from NiMnSb. *Solid State Communications*. 1985;**56**:391
- [44] Patterson F, Moeller C, Ward R. Magnetic Oxides of Molybdenum(V) and Tungsten(V) with the Ordered Perovskite Structure. *Inorganic Chemistry*. 1963;**2**:196

- [45] Galasso F, Douglas FC, Kasper RJ. Relationship Between Magnetic Curie Points and Cell Sizes of Solid Solutions with the Ordered Perovskite Structure. *Journal of Chemical Physics*. 1966;**44**:1672
- [46] Nakagawa T. Magnetic and Electrical Properties of Ordered Perovskite $\text{Sr}_2(\text{FeMo})\text{O}_6$ and Its Related Compounds. *Journal of the Physical Society of Japan*. 1968;**24**:806
- [47] Sleight AW, Longo J, Ward R. Compounds of Osmium and Rhenium with the Ordered Perovskite Structure. *Inorganic Chemistry*. 1962;**1**:245
- [48] Kobayashi KI, Kimura T, Sawada H, Terakura K, Tokura Y. Room-temperature magnetoresistance in an oxide material with an ordered double-perovskite structure. *Nature*. 1998;**395**:677
- [49] Kumar N, Gaur A, Kotnala RK. Stable Fe deficient $\text{Sr}_2\text{Fe}_{1-\delta}\text{MoO}_6$ ($0.0 \leq \delta \leq 0.10$) compound. *Journal of Alloys and Compounds*. 2014;**601**:245
- [50] Kumar N, Khurana G, Gaur A, Kotnala RK. Room temperature low field magnetoresistance in $\text{Sr}_2\text{FeMoO}_6/\text{Zn}_x\text{Fe}_{1-x}\text{Fe}_2\text{O}_4$ composites. *Journal of Applied Physics*. 2013;**114**:053902
- [51] Kumar N, Aloysius RP, Gaur A, Kotnala RK. Study of ferromagnetic-metal type $\text{Sr}_2\text{FeMoO}_6 + x\text{Ag}$ ($x = 0-10$ wt%) composites. *Journal of Alloys and Compounds*. 2013;**559**:64
- [52] Pandey V, Verma V, Bhalla GL, Kotnala RK. Increased low field magnetoresistance in electron doped system $\text{Sr}_{0.4}\text{Ba}_{1.6-x}\text{La}_x\text{FeMoO}_6$. *Journal of Applied Physics*. 2012;**108**:053912
- [53] Sarma DD, Ray S, Tanaka K, Kobayashi M, Fujimori A, Sanyal P, Krishnamurthy HR, Dasgupta C. Intergranular Magnetoresistance in $\text{Sr}_2\text{FeMoO}_6$ from a Magnetic Tunnel Barrier Mechanism across Grain Boundaries. *Physical Review Letters*. 2007;**98**:157205
- [54] Huang YH, Yamauchi H, Karppinen M. Competition between intragranular and intergranular tunneling magnetoresistance in polycrystalline $\text{Sr}_2\text{FeMoO}_6$. *Physical Review B*. 2006;**74**:174418
- [55] Ray S, Middey S, Jana S, Banerjee A, Sanyal P, Rawat R, Gregoratti L, Sarma DD. Origin of the unconventional magnetoresistance in $\text{Sr}_2\text{FeMoO}_6$. *Europhysics Letters*. 2011;**94**:47007
- [56] Jana S, Middey S, Ray S. Spin-valve-type magnetoresistance: a generic feature of ferromagnetic double perovskites. *Journal of Physics: Condensed Matter*. 2010;**22**:346004
- [57] Ji WJ, Xu J, Zhang ST, Chen YB, Jian Z, ZB Gao, S H Yao, Y F Chen, Thickness dependent microstructures and properties of $\text{Sr}_2\text{Fe}_{10/9}\text{Mo}_{8/9}\text{O}_6$ films grown in N_2 . *Solid State Communications*. 2013;**163**:28
- [58] Paturi P, Metsanoja M, Huhtinen H. Optimization of deposition temperature and atmosphere for pulsed laser deposited $\text{Sr}_2\text{FeMoO}_6$ thin films. *Thin Solid Films*. 2011;**519**:8047

- [59] Jalili H, Heinig NF, Leung KT. Growth evolution of laser-ablated $\text{Sr}_2\text{FeMoO}_6$ nanostructured films: Effects of substrate-induced strain on the surface morphology and film quality. *Journal of Chemical Physics*. 2010;**132**:204701
- [60] Suominen T, Raittila J, Paturi P. Pure and fully texturized $\text{Sr}_2\text{FeMoO}_6$ thin films prepared by pulsed laser deposition from target made with citrate-gel method. *Thin Solid Films*. 2009;**517**:5793
- [61] Fix T, Barla A, Ulhaq-Bouillet C, Colis S, Kappler JP, Dinia A. Absence of tunnel magnetoresistance in $\text{Sr}_2\text{FeMoO}_6$ -based magnetic tunnel junctions. *Chemical Physics Letters*. 2007;**434**:276
- [62] Boucher R. $\text{Sr}_2\text{FeMoO}_{6+x}$: Magnetic and electrical property dependence on thickness and substrate type. *Journal of Magnetism and Magnetic Materials*. 2006;**301**:251
- [63] Song JH, Park JH, Jeong YH. Achieving large magnetoresistance in $\text{Sr}_2\text{FeMoO}_6$ thin films. *Journal of Applied Physics*. 2005;**97**:046105
- [64] Fix T, Stoeffler D, Colis S, Ulhaq C, Versini G, Vola JP, Huber F, Dinia A. Effects of strain relaxation on the electronic properties of epitaxial $\text{Sr}_2\text{FeMoO}_6$ grown by pulsed laser deposition on SrTiO_3 (001). *Journal of Applied Physics*. 2005;**98**:023712
- [65] Sanchez D, Garcia-Hernandez M, Auth N, Jakob G. Structural, magnetic, and transport properties of high-quality epitaxial $\text{Sr}_2\text{FeMoO}_6$ thin films prepared by pulsed laser deposition. *Journal of Applied Physics*. 2004;**96**:2736
- [66] Kim DY, Kim JS, Park BH, Lee JK, Kim JH, lee JH, Chang J, Kim HJ. SrFeO_3 nanoparticles-dispersed SrMoO_4 insulating thin films deposited from $\text{Sr}_2\text{FeMoO}_6$ target in oxygen atmosphere. *Applied Physics Letters*. 2004;**84**:5037
- [67] Shinde SR, Ogale SB, Greene RL, Venkatesan T, Tsoi K, Cheong SW, Millis AJ. Thin films of double perovskite $\text{Sr}_2\text{FeMoO}_6$: Growth, optimization, and study of the physical and magnetotransport properties of films grown on single-crystalline and polycrystalline SrTiO_3 substrates. *Journal of Applied Physics*. 2003;**93**:1605
- [68] Bibes M, Bouzehouane K, Besse M, Barthelemy A, Fusil S, Bowen M, Seneor P, Contour JP, Fert A. Tunnel magnetoresistance in nanojunctions based on $\text{Sr}_2\text{FeMoO}_6$. *Applied Physics Letters*. 2003;**83**:2629
- [69] Santiso J, Fraxedas J, Balcells L, Fontcuberta J, Figueras A. In situ characterisation of $\text{Sr}_2\text{FeMoO}_6$ films prepared by pulsed laser deposition, *J. Phys. IV France*, 11 PR11 (2001) Pr11-307
- [70] Westerburg W, Reisinger D, Jakob G. Epitaxy and magnetotransport of $\text{Sr}_2\text{FeMoO}_6$ thin films. *Physical Review B*. 2000;**62**:R767
- [71] Manako T, Izumi M, Konishi Y, Kobayashi KI, Kawasaki M, Tokura Y. Epitaxial thin films of ordered double perovskite $\text{Sr}_2\text{FeMoO}_6$. *Applied Physics Letters*. 1999;**74**:2215
- [72] Santiso J, Figueras A, Fraxedas J. Thin films of $\text{Sr}_2\text{FeMoO}_6$ grown by pulsed laser deposition: preparation and characterization. *Surface and Interface Analysis*. 2002;**33**:676

- [73] Venimadhav A, Sher F, Attfield JP, Blamire MG. Oxygen assisted deposition of $\text{Sr}_2\text{FeMoO}_6$ thin films on $\text{SrTiO}_3(100)$. *Journal of Magnetism and Magnetic Materials*. 2004;**269**:101
- [74] Venimadhav A, Vickers M, Blamire M. Ferromagnetic spin ordering in disordered $\text{Sr}_2\text{FeMoO}_6$ films. *Solid State Communications*. 2004;**130**:631
- [75] Borges RP, Lhostis S, Bari MA, Versluijs JJ, Lunney JG, Coey JMD, Besse M, Contour JP. Thin films of the double perovskite $\text{Sr}_2\text{FeMoO}_6$ deposited by pulsed laser deposition. *Thin Solid Films*. 2003;**429**:5
- [76] Asano H, Ogale SB, Garrison J, Orozco A, Li YH, Li E, Smolyaninova V, Galley C, Downes M, Rajeswari M, Ramesh R, Venkatesan T. Pulsed-laser-deposited epitaxial $\text{Sr}_2\text{FeMoO}_6-y\text{Sr}_2\text{FeMoO}_6-y$ thin films: Positive and negative magnetoresistance regimes. *Applied Physics Letters*. 1999;**74**:3696
- [77] Besse M, Pailloux F, Barthelemy A, Bouzehouane K, Fert A, Olivier J, Durand O, Wyczisk F, Bisaro R, Contour JP. Characterization methods of epitaxial $\text{Sr}_2\text{FeMoO}_6$ thin films. *Journal of Crystal Growth*. 2002;**241**:448
- [78] Sanchez D, Auth N, Jakob G, Martinez JL, Garcia-Hernandez M, et al. Pulsed laser deposition of $\text{Sr}_2\text{FeMoO}_6$ thin films. *Journal of Magnetism and Magnetic Materials*. 2005;**294**:e119
- [79] Fix T, Versini G, Loison JL, Colis S, Schmerber G, Pourroy G, Dinia A. Pressure effect on the magnetization of $\text{Sr}_2\text{FeMoO}_6$ thin films grown by pulsed laser deposition. *Journal of Applied Physics*. 2005;**97**:024907
- [80] Yin HQ, Zhou JS, Zhou JP, Dass R, McDevitt JT, Goodenough JB. Intra- versus intergranular low-field magnetoresistance of $\text{Sr}_2\text{FeMoO}_6/\text{Sr}_2\text{FeMoO}_6$ thin films. *Applied Physics Letters*. 1999;**75**:2812
- [81] Trolio AD, Larciprete R, Testa A, Fiorani D, Imperatori P, Turchini S, Zema N. Double perovskite $\text{Sr}_2\text{FeMoO}_6/\text{Sr}_2\text{FeMoO}_6$ films: Growth, structure, and magnetic behavior. *Journal of Applied Physics*. 2006;**100**:0139071
- [82] Wang S, Pan H, Zhang X, Lian G, Xiong G. Double-perovskite $\text{Sr}_2\text{FeMoO}_6$ epitaxial films with ordered cation structure grown in mixture gas of hydrogen and argon. *Applied Physics Letters*. 2006;**88**:121912
- [83] Song JH, Park BG, Park JH, Jeong YH. Double-Perovskite $\text{Sr}_2\text{FeMoO}_6$ Thin Films Prepared by Using Pulsed Laser Deposition: Growth and Crystal, Electronic and Magnetic Structures. *Journal of the Korean Physical Society*. 2008;**53**:1084
- [84] Jalili H, Heinig NF, Leung KT. X-ray photoemission study of $\text{Sr}_2\text{FeMoO}_6$ and SrMoO_4 films epitaxially grown on $\text{MgO}(001)$: Near-surface chemical-state composition analysis. *Physical Review B*. 2009;**79**:174427
- [85] Saloaro M, Majumdar S, Huhtinen H, Paturi P. Absence of traditional magnetoresistivity mechanisms in $\text{Sr}_2\text{FeMoO}_6$ thin films grown on SrTiO_3 , MgO and NdGaO_3 substrates. *Journal of Physics: Condensed Matter*. 2012;**24**:366003

- [86] Asano H, Kohara Y, Matsui M. Coherent Epitaxy and Magnetic Properties of $\text{Sr}_2\text{FeMoO}_6$ Thin Films on $\text{Ba}_{0.4}\text{Sr}_{0.6}\text{TiO}_3$ -Buffered SrTiO_3 Substrates. *Japanese Journal of Applied Physics*. 2002;**41**:L1081
- [87] Metsanoja M, Majumdar S, Huhtinen H, Effect of ex situ post-annealing treatments on $\text{Sr}_2\text{FeMoO}_6$ thin films. *Journal of Superconductivity and Novel Magnetism*. 2012;**25**:829
- [88] Asano H, Koduka N, Imaeda K, Sugiyama M, Matsui M. Magnetic and junction properties of half-metallic double-perovskite thin films. *IEEE Transactions on Magnetics*. 2005;**41**:2811
- [89] Fix T, Stoeffler D, Henry Y, Colis S, Dinia A, Dimopoulos T, Bär L, Wecker J. Diode effect in all-oxide $\text{Sr}_2\text{FeMoO}_6$ -based magnetic tunnel junctions. *Journal of Applied Physics*. 2006;**99**:08J107
- [90] Jalili H, Heinig NF, Leung KT. Formation of nanocrystalline films of $\text{Sr}_2\text{FeMoO}_6/\text{Sr}_2\text{FeMoO}_6$ on Si(100) by pulsed laser deposition: Observation of preferential oriented growth. *Journal of Applied Physics*. 2009;**105**:034305
- [91] Bianchini L. Synthesizing and characterizing $\text{Sr}_2\text{FeMoO}_6$ bulk and thin films. *Undergraduate Review*. 2008;**4**:65
- [92] Kim DY, Kim JS, Park BH, Lee JK, Kim JH, lee JH, Chang J, Kim HJ. I Kim, Y D Park, SrFeO_3 nanoparticles-dispersed SrMoO_4 insulating thin films deposited from $\text{Sr}_2\text{FeMoO}_6$ target in oxygen atmosphere. *Applied Physics Letters*. 2004;**84**:5037
- [93] Hernandez MG, Martinez JL, Martinez-Lope MJ, Casais MT, Alonso JA. Finding Universal Correlations between Cationic Disorder and Low Field Magnetoresistance in FeMo Double Perovskite Series. *Physical Review Letters*. 2001;**86**:2443
- [94] Yin HQ, Zhou JS, Dass R, Zhou JP, McDevitt JT, Goodenough JB. Grain-boundary room-temperature low-field magnetoresistance in $\text{Sr}_2\text{FeMoO}_6$ films. *Journal of Applied Physics*. 2000;**87**:6761
- [95] Brinkman WF, Dynes RC, Rowell JM. Tunneling Conductance of Asymmetrical Barriers. *Journal of Applied Physics*. 1970;**41**:1915
- [96] Bowen M, Bibes M, Barthelemy A, Contour JP, Anane A, Lemaitre Y, Fert A. Nearly total spin polarization in $\text{La}_{2/3}\text{Sr}_{1/3}\text{MnO}_3/\text{La}_{2/3}\text{Sr}_{1/3}\text{MnO}_3$ from tunneling experiments. *Applied Physics Letters*. 2003;**82**:233
- [97] Julliere M. Tunneling between ferromagnetic films. *Physics Letters A*. 1975;**54**:225
- [98] Muduli PK, Budhani RC, Topwal D, Sarma DD. Spin-polarized electron tunneling in polycrystalline $\text{Sr}_2\text{FeMoO}_6$ thin films. *Journal of Physics: Conference Series*. 2009;**150**:042132